

Optimal Quench for Distance-Independent Entanglement and Maximal Block Entropy

Bedoor Alkurtass,^{1,2} Leonardo Banchi,¹ and Sougato Bose¹

¹*Department of Physics and Astronomy, University College London, Gower Street, WC1E 6BT London, United Kingdom*

²*Department of Physics and Astronomy, King Saud University, Riyadh 11451, Saudi Arabia*

(Dated: June 5, 2022)

We optimize a quantum walk of multiple fermions following a quench in a spin chain to generate near ideal resources for quantum networking. We first prove an useful theorem mapping the correlations evolved from specific quenches to the apparently unrelated problem of quantum state transfer between distinct spins. This mapping is then exploited to optimize the dynamics and produce large amounts of entanglement distributed in very special ways. Two applications are considered: the simultaneous generation of many Bell states between pairs of distant spins (maximal block entropy), or high entanglement between the ends of an arbitrarily long chain (distance-independent entanglement). Thanks to the generality of the result, we study its implementation in different experimental setups using present technology: NMR, ion traps and ultracold atoms in optical lattices.

I. INTRODUCTION

Entanglement is an essential resource for linking distinct quantum registers through teleportation [1]. Therefore, the generation and distribution of entanglement over distances long enough to link separated quantum units on a chip is becoming topical [2–7]. In parallel, the spread/growth of entanglement from unentangled states due to a quench has become a topic of great interest in condensed matter, both theoretically [8–22] and experimentally [23, 24]. Could it be used for the practical purpose of connecting quantum registers, especially in view of its experimental viability [23–25]? This is largely unexplored as the entanglement generated in typical quenches is between blocks and is *not* arranged in the special form of a high entanglement between individual spin pairs. Such block-block entanglement is not readily useful for applications such as connecting quantum registers. Moreover, whether two large complementary parts of a spin chain can get *maximally* entangled through a quench with no further manipulation/control is not known to date. Here we show that a simple global quench of a Hamiltonian with spatially varying couplings can not only yield maximal entanglement between complementary blocks of a spin chain, but this entanglement is also distributed in the special form of singlet states of individual pairs of spins. This state is a resource for many simultaneous entangling gates between pairs of quantum registers. From a condensed matter perspective, we show that *unbounded* entanglement (a topic of high interest [20]) can be obtained even in non-interacting systems with suitably engineered interactions.

Entanglement between extremal spins of a chain is currently a topic of active interest because of its linking power [26–34]. However, whether fast (non-adiabatic) dynamics following a “global” quench can produce *distance-independent* entanglement between extremal spins of a chain is an open question. In schemes studied so far, it typically falls off with the length of the chain [30–33]. This task is, of course, less demanding than maximal entanglement between two complementary blocks. As a second result, we show that distance independent entanglement can be achieved with quenches to Hamiltonians with “minimal” spatial variation of couplings.

Our study is also motivated by some recent experimental

activities. Multipartite quantum walks have recently gathered exceptional interest [35] fueled largely by the inefficiency of the classical simulation of many-boson quantum walks [36]. The spin chain we consider can be mapped into a fermion hopping model, so the quench generates a many-fermion quantum walk. Many-fermion quantum walks, on the other hand, can be efficiently simulated classically [37] – so one might naively assume them to be of no advantage to quantum information processing. In that respect, what we find here is interesting – the many fermion quantum walk can still generate resources for quantum information tasks, and produce a maximal amount of entanglement. Another subject of high experimental interest is the spread of quantum correlations after a quench [23, 24, 38]. Our work is aimed at offering possibilities to take these studies beyond their fundamental remit, namely in “optimizing” these correlations for useful purposes.

In this article we consider the quench that evolves an initial Néel or ferromagnetic state according to an appropriate free fermion spin model in 1D with the possibility of a spatial variation of the spin-spin couplings. First we prove a mapping which relates the resulting many-fermion quantum walk to a simpler dynamics: we show that correlations developing between two sites m, n at a time $t/2$ after the quench is related to amplitude of single walker to travel from m to n in a time t . The difference in the times is noteworthy, and highlights the non-triviality of the result (we are *not* merely restating the well known resolvability of the many free fermion walk to simultaneous single particle walks). Such continuous time quantum walks of a single walker has been subject to intensive research in recent years, motivated by the understanding of quantum information transfer [39] and quantum computation [40]. Our new mapping between quench and quantum walk, together with the wealth of results about information transmission, allows us to propose different optimal strategies to dynamically generate entanglement between distant sites, simultaneously. In particular, exploiting Hamiltonians which allow perfect transmission [41], one can generate with the quench a maximal set of Bell states between distant spins and ultimately maximal block entropy. A similar final state was obtained in [42] using a combination of Ising-like interactions in two different directions in alternate sites. Our method is conceptually simpler, as it requires the same type of cou-

pling throughout the chain. On the other hand, Hamiltonians allowing *almost*-perfect transfer are easier to implement experimentally, as they usually require a static tuning of a single parameter [43–46] rather than a full-engineering. We show that these models allow the generation a high entanglement between the ends of the chain, in principle even for $N \rightarrow \infty$ (*i.e.*, distance independent entanglement).

II. MAPPING BETWEEN QUENCH AND STATE TRANSFER

We consider a chain of N spin- $\frac{1}{2}$ particles coupled by the following Hamiltonian

$$\mathcal{H}_\Delta = \frac{J}{2} \sum_{n=1}^N \left[j_n (\sigma_n^x \sigma_{n+1}^x + \sigma_n^y \sigma_{n+1}^y) + \Delta \sigma_n^z \sigma_{n+1}^z \right], \quad (1)$$

where σ_n^α are the Pauli matrices, $J j_n$ are the coupling strengths (J is the energy unit, while j_n are adimensional) and Δ is the eventual anisotropy. We are interested in the entanglement generation via the non-equilibrium evolution of the Néel initial state $|\text{AFM}\rangle = |\uparrow\downarrow\uparrow\downarrow\dots\rangle$ under the XX Hamiltonian $\mathcal{H}_{\Delta=0}$. Formally this corresponds to a quench from $\Delta=\infty$ to $\Delta=0$, though the state $|\text{AFM}\rangle$ can be prepared in different ways [47].

We now prove a theorem which connects the many-body non-equilibrium evolution following the quench to a state transfer problem. This connection will be then exploited to maximize the amount of generated entanglement. The Hamiltonian \mathcal{H}_0 can be mapped to a fermionic hopping Hamiltonian via the Jordan-Wigner (JW) transformation $c_n^\dagger = \prod_{m<n} (-\sigma_m^z) \sigma_n^+$, $\sigma_n^+ = [\sigma_n^x + i\sigma_n^y]/2$: the new operators obey fermionic anti-commutation relations $\{c_n, c_m^\dagger\} = \delta_{nm}$, and $\mathcal{H}_0 = \sum_{nm} A_{nm} c_n^\dagger c_m$. The initial state $|\text{AFM}\rangle$ has a fixed number of “particles” and \mathcal{H}_0 is quadratic and particle-conserving. Thus, owing to Wick’s theorem, the evolved state is completely specified in the Heisenberg picture by the two-point correlation functions $\langle c_n^\dagger(t) c_m(t) \rangle$ where $\langle \cdot \rangle = \langle \text{AFM} | \cdot | \text{AFM} \rangle$. It is $\langle c_n^\dagger(t) c_m(t) \rangle = \sum_{ij} f_{ni}^*(t) f_{mj}(t) \langle c_i^\dagger c_j \rangle$ where $f = e^{-itA}$, in matrix notation. By defining the sign matrix $S_{ij} = (-1)^{i+1} \delta_{ij}$ we find that $\langle c_i^\dagger c_j \rangle = (\delta_{ij} + S_{ij})/2$ and since A is tri-diagonal, $SAS = -A$. Thus we obtain the following equality

$$\langle c_n^\dagger(t) c_m(t) \rangle = \frac{\delta_{nm} + (-1)^{n+1} f_{nm}(2t)}{2}, \quad (2)$$

for any pair of sites n, m . Before clarifying the implications of Eq. (2), we note that $f_{nm}(t)$ represents the probability amplitude for a fermionic quantum walker to reach site n at time t , starting from site m . In the single-particle sector, the fermionic nature of the walker does not show up, and $|f_{nm}(t)|^2$ quantifies also the state transmission probability from m to n of spin $|\uparrow\rangle$ traveling in a “sea” of $|\downarrow\rangle$ spins. Therefore, if the Hamiltonian (1) for a particular set of couplings $\{j_n\}$ allows perfect single-excitation transfer from m to n at some time t^* , then starting from the many-body $|\text{AFM}\rangle$ initial state two fermions get completely delocalized among the two distant sites m, n at time $t^*/2$, *i.e.* half of the transmission time. By

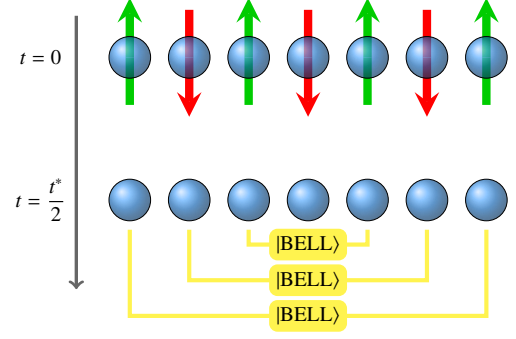


FIG. 1. (Color online) Schematic picture for dynamical generation of entanglement using a fully engineered XX Hamiltonian and the Néel initial state.

taking into account the non-local relation between fermions and spins, in the following we prove that at time $t^*/2$ the sites m, n get maximally entangled for particular Hamiltonians and pairs of spins. Therefore, Eq.(2) relates the dynamical entanglement generation from the quench to a simpler optimization of independent quantum walks.

We conclude this introductory discussion with a further comment on Eq. (2), to avoid confusions with Rabi-like dynamics. Two qubits interacting via an XX Hamiltonian with coupling J , display perfect state transfer ($|\uparrow\downarrow\rangle \rightarrow |\downarrow\uparrow\rangle$) after a time $t^* = \pi/(2J)$ and a Bell state generation ($\sqrt{2}|\uparrow\downarrow\rangle \rightarrow |\uparrow\downarrow\rangle - i|\downarrow\uparrow\rangle$) after a time $t^*/2$. However, the interpretation of Eq. (2) as a long distance version of this behaviour is wrong. If a ballistic transfer happens on a time t^* , the distant spins cannot be entangled by a single traveling particle after $t^*/2$: this would violate the Lieb-Robinson bound [48]. The physical explanation of the effect we describe is that each $|\uparrow\rangle$ in the initial states propagates in the two different directions and contributes a certain amount of entanglement between the spins in its effective “light cone” [8]. However, a *single*, delocalized, hopping particle cannot produce maximal long distance entanglement. The final amount of entanglement is due to the sum of different contributions given by each counter-propagating quasi-particle. Therefore, the maximal entanglement generation presented in this article is a truly many-particle effect, which arguably depends on the particular alternation of spins $|\uparrow\rangle$ and $|\downarrow\rangle$ in the Néel initial state [30, 31],

A. Fully engineered Hamiltonians for maximal block entropy

Perfect transmission can be achieved via engineered Hamiltonians such as the XX chain with couplings $j_n = \sqrt{n(N-n)}/N$ [49, 50]. In this engineered chain any walker starting from n is exactly transmitted to its mirror symmetric position $N-n+1$ at the transmission time $t^* = \pi N/(2J)$. Thanks to the mapping Eq. (2), we show that, when the chain is initially set in the (separable) Néel state, after a time $t^*/2$ the state evolves into a maximal set of *nested* Bell states. A schematic picture of this process is shown in Fig. 1. As $|f_{n, N-n+1}(t^*)| = 1$ for any n , it is $|\Xi\rangle = e^{-i\mathcal{H}_0 t^*/2} |\text{AFM}\rangle \propto (c_1^\dagger + e^{i\alpha_1} c_N^\dagger)(c_2^\dagger + e^{i\alpha_2} c_{N-1}^\dagger) \dots |0\rangle$, be-

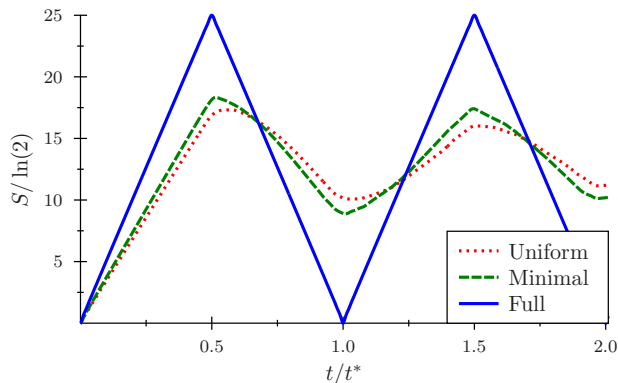


FIG. 2. (Color online) Entropy dynamics for fully engineered, minimal engineered and uniform couplings. $N=51$.

ing $|0\rangle$ the vacuum of the fermi operators and α_i some defined phases. In $|\Xi\rangle$ the spin in position n is maximally entangled with the one in position $N-n+1$, as in Fig. 1. Indeed, $c_n^\dagger \propto \sigma_n^+$ up to a phase which depends on the number of spin $|\uparrow\rangle$ in position $m < n$. Proceeding recursively from the center of the chain, one can show that $|\Xi\rangle \propto (\sigma_1^+ + e^{i\alpha_1} \sigma_N^+) (\sigma_2^+ + e^{i\alpha_2} \sigma_{N-1}^+) \dots |0\rangle$, for some new phases α'_n . In appendix A we prove that $\alpha'_n = \alpha$, so the generated Bell states are $|\text{BELL}\rangle = (|\downarrow\uparrow\rangle + e^{i\alpha} |\uparrow\downarrow\rangle) / \sqrt{2}$, being $\alpha=0$ for N odd and $\alpha=\pi/2$ for N even. Accordingly, the left block of the chain is maximally entangled with the right block. The corresponding dynamics of the entropy is shown in Fig. 2. Finally, our method is much more efficient to generate pairs of remote maximally entangled states. Indeed, the operational time of our protocol scales as N , while the generation of the same state via a composition of CNOT and SWAP gates would require a number of operations of the order of $N \times N$.

B. Minimally engineered model for distance-independent entanglement

Minimally engineered chains [43–45] allows an optimal ballistic transmission between the chain boundaries. Here only a single parameter is tuned, i.e. the couplings $j_1 = j_{N-1} = j'$ at the ends. The other qubits are uniformly coupled with $j_n = 1/2$, $n \neq 1, N-1$. When j' is set to an optimal value $\propto N^{-1/6}$ the dynamics is ruled by the excitations with linear dispersion relation [45]. Thus $|f_{N1}(t^*)| \approx 1$ for a ballistic transmission time $t^* \approx N/v$, being $v \approx J$ the group velocity.

Minimal engineering maximizes the transmission quality between the chain ends, without optimizing the transmission between other pairs. After the quench, we know from Eq. (2) that at time $t^*/2$ there is an almost-maximally delocalized fermion \tilde{c} between the two ends. Since $c_N^\dagger = \sigma_N^+ \Pi$, where the parity Π of the whole chain is a constant of motion and $\Pi|\text{AFM}\rangle = \pm|\text{AFM}\rangle$, the fermion \tilde{c} yields a highly entangled state between the ends of the chain. However, in this case $|f_{N1}(t^*)| \neq 1$ because the fermion \tilde{c} has a non-zero probability of staying far from the ends, so the generated long-distance entangled state $\rho_{1,N}$ is not maximally entangled. The amount of entanglement is quantified by the fully entangled

fraction $F(t) = \max_{|e\rangle} \langle e | \rho_{1,N}(t) | e \rangle$, where $|e\rangle$ is a maximally entangled states. When $F > \frac{1}{2}$ the state is purifiable (hence useful for teleportation [51]). We found $F(t) = (1 + |f_{N1}(2t)|)^2 / 4$. When the optimal $j'(N)$ is used, $|f_{N1}(t^*)| \approx 85\%$ for $N \rightarrow \infty$ [45]. Therefore the generated entangled state is almost distance-independent as $F > 85\%$ even in the infinite site limit. Minimal engineering increases the resulting entanglement significantly compared to the uniform case [30]. For smaller chains F is fairly larger (see appendix B) and, e.g., for $N=25$ it is $F=97\%$.

C. Quench from other initial states

All the results discussed so far can be obtained also with the following Hamiltonian

$$\mathcal{H}'_B = \frac{J}{2} \sum_{n=1}^N j_n (\sigma_n^x \sigma_{n+1}^x - \sigma_n^y \sigma_{n+1}^y) - B \sum_n \sigma_n^z, \quad (3)$$

by quenching the magnetic field from $B=\infty$ to $B=0$. The initial state in this case is $|\text{FM}\rangle = |\uparrow\uparrow\uparrow \dots\rangle$ and $e^{-i\mathcal{H}'_0 t} |\text{FM}\rangle = \prod_{n \text{ even}} \sigma_n^x e^{-i\mathcal{H}'_0 t} |\text{AFM}\rangle$. As $\prod_{n \text{ even}} \sigma_n^x$ is a product of local rotations, the states $e^{-i\mathcal{H}'_0 t} |\text{AFM}\rangle$ and $e^{-i\mathcal{H}'_0 t} |\text{FM}\rangle$ share the same amount of entanglement.

In appendix C we study also the quench from a different initial state (series of nearest-neighbor Bell states) that might be easier to generate in some experimental setups [52].

III. EXPERIMENTAL PROPOSALS

A. NMR-based implementation

Pulsed control techniques in Nuclear Magnetic Resonance (NMR) have reached a high degree of maturity [53] and provide a platform to observe quantum dynamics and state transfer in spin chains [54, 55]. The natural dipolar interactions between the nuclear spins can be tuned [56, 57] and an effective “double-quantum” Hamiltonian (3) obtained. In particular, a suitable pulse sequence to engineer the coupling strengths according to $j_n = \sqrt{n(N-n)}/N$ has been recently proposed [57]. At $t^* = \pi N / (2J)$, where $J \approx 5$ KHz, a nearly lossless state transfer is expected for chains as long as $N=25$ [57]. Owing to our mapping, a near perfect generation of *nested* Bell states is expected when an initially polarized state $|\text{FM}\rangle$ evolves under \mathcal{H}'_0 for a time $t^*/2$. In the high temperature regime, a *pseudo-pure* initial state $\rho_{\text{pp}} = \frac{\zeta}{2N} \mathbb{1} + (1-\zeta) |\text{FM}\rangle \langle \text{FM}|$ may be implemented using standard averaging techniques if enough control on the spins is available [58–60]. The initialization error ζ leads to $F = 1 - 3\zeta/4$. When ζ is low we have actual entanglement, while when it is high the correlations enable one to verify the protocol. The spins at the ends can be read out [61] exploiting their peculiarity of having just one nearest neighbor. The main error sources are typically pulse errors and intra-chain interactions [56]. For simplicity, we model these errors as an imperfect filtered engineering [57] of \mathcal{H}'_B . We consider $\tilde{\mathcal{H}}' = J \sum_{n \neq m} A_{nm} (\sigma_n^x \sigma_m^x - \sigma_n^y \sigma_m^y)$,

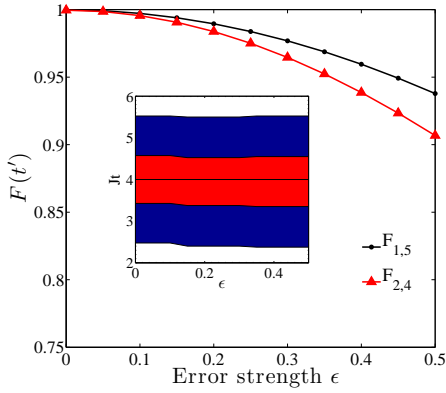


FIG. 3. (Color online) Fully entangled fraction $F_{n,N-n+1}(t')$ for pairs of mirror symmetric spins at the time $t' \approx t^*/2$ which maximizes $F_{1,N}$, $N=5$. For $N=5$ fully and minimally engineered chains coincide. The pulse error ϵ is defined in the text. An average over 100 realizations of the imperfections is considered. Inset: t' (black line), time where $F_{1,5} \geq 0.9 F_{1,5}(t')$ (red or light gray area), time where $F_{1,5} \geq 0.5 F_{1,5}(t')$ (blue or dark gray area).

$A_{nm} = j_n(\delta_{n,m+1} + \delta_{n+1,m}) + \epsilon b_{nm} F_{nm}$ where ϵ is the error strength, b_{nm} models the long range interactions and F models the imperfect filtering. To include the effect of a nearby chain, we consider two parallel chains coupled via dipolar interaction b_{nm} , where the interchain distance is three times the distance between intrachain spins [56]. The elements $F_{nm} \in [-1, 1]$ are chosen at random. The results are shown in Fig. 3.

B. Ion Traps Implementation

Ion traps represent a promising implementation of a quantum computer where two internal hyperfine states of each trapped ion implement a qubit [62–64]. Ising-like coupling between ions can be induced using a magnetic field gradient [65, 66]. In addition, the magnetic field gradient causes local frequency shifts allowing for addressing and manipulation of individual ions using microwave pulses. Segmented microstructured traps provide the possibility of tailoring the couplings via local trapping potential, thus allowing for suppression of long-range couplings [66]. Alternatively, spin-spin coupling can be generated by laser-induced forces [23, 24, 67]. An effective XX Hamiltonian can be implemented either with a large transverse magnetic field [23] or via fast sequential applications of Ising evolution in two orthogonal directions [29]. The main sources of error here are long-range interactions and dephasing. The robustness of our scheme against decoherence is studied in Fig. 4 in terms of the dephasing rate $J\gamma$. As $J \approx 1$ kHz [29] we find that with a decoherence time $1/(J\gamma) \approx 100$ ms the entangled fraction F can be higher than 80% for $N = 10$ (dynamical decoupling as in Ref. [68] can be used as our scheme is invariant to π pulses). To study the effect of long-range interactions we use the approximation $j_{nm} = (\omega_n^2 \omega_m^2 |n - m|^3)^{-1}$, valid when the Coulomb interaction is a perturbation of the trapping potential (see e.g.

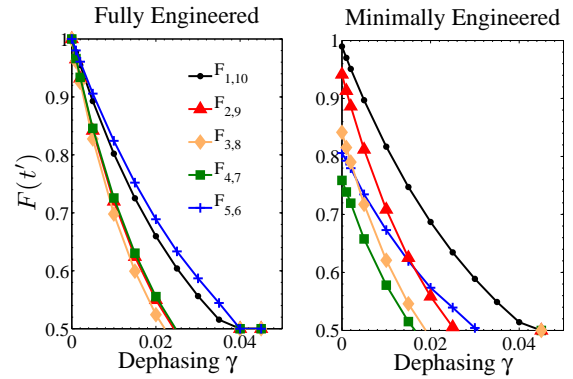


FIG. 4. (Color online) $F_{n,N-n+1}(t')$ as in Fig. 3. Fully engineered (left) and minimally engineered (right) chains for $N=10$. Decoherence is modeled by the master equation $\dot{\rho} = -i[\mathcal{H}_0, \rho] + J\gamma \sum_i (\sigma_i^z \rho \sigma_i^z - \rho)$ with dephasing rate γ [29].

$F_{n,N-n+1}(t')$	$n = 1$	$n = 2$	$n = 3$	$n = 4$	$n = 5$
Fully engineered	0.88	0.82	0.83	0.85	0.88
Minimally engineered	0.88	0.77	0.69	0.57	0.60

TABLE I. Fully entangled fraction with long range interactions, where $t' \approx t^*/2$, $N=10$.

[67, 69]); ω_n is the frequency of the local trap, chosen such that $j_{n,n+1} = j_n$. The result is displayed in Table. I.

C. Optical lattice implementation

In optical lattices, the qubit is encoded into two hyperfine states of a neutral atom [52, 70, 71]. Nearly all requirements for the implementation of our scheme have been met in Refs. [25, 72] – for example, lines of 10-14 atoms without defects forming a spin chain can be post-selected using a quantum gas microscope, which can also be used to readout individual atomic state to verify the generated entanglement. The Néel state initialization should be possible by preparing a spin polarized state and flipping alternate spins by combined action of light from a spatial light modulator (SLM) and a resonant microwave pulse in exactly the same manner as a single [72] and double [25] rows of spins were selectively flipped in recent experiments. After the initialization, one should suddenly (in $\ll 0.1$ s) change the laser field from the SLM to that with an appropriate intensity profile [73] to generate the effective coupling j_n , as well as to provide a hard wall end to the lattice [6]. An effective XX Hamiltonian with $J \approx 50$ Hz, should be possible by tuning (e.g. by Feshbach resonance) interspecies and intraspecies interactions [74]. On the other hand, experimental imperfectnesses can introduce spurious interactions as an effective anisotropic $J_z \sigma_n^z \sigma_{n+1}^z$ term. We found that the entangling scheme is robust against these imperfections, with 90% of the entanglement preserved for upto $J_z \approx 0.35 j_n$.

IV. CONCLUSIONS

We have mapped the correlations between two spins m, n produced by specific quenches at t to a different dynamics, namely a spin transfer between sites m and n at $2t$. This non-trivial mapping allows one to generate both unbounded block-block and useful spin-spin entanglement from a global quench in contrast to much condensed matter literature. We found that a full or a minimal engineering of the couplings simultaneously generates many Bell states (maximal block entropy) or distance-independent entanglement. Our method is much more efficient than a composition of CNOT and SWAP gates to generate a full set of Bell pairs: the former scales as $t \sim N$ while the latter requires $t \sim O(N^2)$. Finally, we have studied the feasibility of realizations in NMR, ion traps and ultracold atoms in optical lattices. Given the sub-decoherence operational times (\approx ms) and the low control required, our method should be competitive for linking quantum registers.

V. ACKNOWLEDGEMENTS

Discussions with Abolfazl Bayat, Paola Cappellaro, Takeshi Fukuhara and Christof Wunderlich are warmly acknowledged. SB and LB are supported by the ERC grant PA-COMANEDIA. BA is supported by King Saud University.

Appendix A: Proof of maximal generation of Bell states

In this section we show that, using a full engineered chain one can generate a maximal set of long-distance bell states as in Fig. 1. For small enough N , one can evaluate efficiently the evolved state exploiting the Fermionic nature of the XX evolution. The time evolved state can indeed be written in a determinant form [43]

$$e^{-i\mathcal{H}_0 t} |m_1, m_2, \dots\rangle = \sum_{\ell_1 < \ell_2 < \dots} \det [f_{(\ell_1, \ell_2, \dots), (m_1, m_2, \dots)}(t)] |\ell_1, \ell_2, \dots\rangle \quad (\text{A1})$$

where $|m_1, m_2, m_3, \dots\rangle$ represents a state with a spin $|\downarrow\rangle$ in positions $m_1 < m_2 < m_3 \dots$, and $f_{(\ell_1, \ell_2, \dots), (m_1, m_2, \dots)}(t)$ is the submatrix of f with rows specified by the index vector (ℓ_1, ℓ_2, \dots) , and columns specified by (m_1, m_2, \dots) .

The matrix elements $f_{nm}(t)$ can be calculated analytically. One can show [49] indeed that

$$f_{n'n}(t) = \langle r' | e^{-i\frac{2t}{N} \mathcal{S}_x^{(s)}} | r \rangle, \quad (\text{A2})$$

where

$$s = \frac{N-1}{2} \quad r = -s + n - 1 \quad r' = -s + n' - 1. \quad (\text{A3})$$

Namely, the engineered quantum walk is equivalent to the rotation of an effective spin- $\frac{N-1}{2}$ along the x direction. Owing to this equivalence the time evolution can be expressed in terms

of the Wigner \mathcal{D} matrix [75]:

$$f_{n'n}(t) = \mathcal{D}_{m'm}^{(s)} \left(\frac{\pi}{2}, -\frac{2t}{N}, -\frac{\pi}{2} \right), \quad (\text{A4})$$

where the definitions (A3) have been used. The matrix elements of the Wigner matrix are well known. For instance, from

$$f_{n'n}(t^*) = (-i)^{N-1} \delta_{n', N-n+1}, \quad (\text{A5})$$

it is now clear that the engineered chain acts as a perfect mirror after a time $t^* = N\pi/2$. However, the analytical expression for $t = t^*/2$ is not so simple.

We prove the structure of Fig. 1 thanks to Eq. (2). Indeed, owing to Wick's theorem, the evolved state can be completely specified by its two point correlation function, up to a global phase. Let us set $N = 2M - 1$ for odd N or $N = 2M$ for even N and

$$e^{-i\mathcal{H}_0 t} |\text{AFM}\rangle = \prod_{k=1}^M \left(\sum_n U_{nk}(t) c_n^\dagger \right) |0\rangle. \quad (\text{A6})$$

Clearly one can set $U_{n1} = f_{n1}^*$, $U_{n2} = f_{n3}^*$, $U_{n3} = f_{n5}^*$, etc., so that the result is (A1). However, there is some arbitrary freedom in choosing U : also with a different $M \times N$ matrix U the result can still be that of (A1). We exploit this arbitrariness in order to simplify the derivation. By calculating $R_{nm}(t) = \langle c_n(t) c_m^\dagger(t) \rangle$ with the ansatz (A6) one finds

$$R_{nm}(t) = \det [U^{(n)\dagger} U^{(m)}], \quad (\text{A7})$$

where $U^{(m)}$ is built from U by adding the column vector $e^{(m)}$ which has only one non-zero element, $(e^{(m)})_m = 1$. Then R_{nm} can be written as a determinant of a $(M+1) \times (M+1)$ matrix in a block form

$$R_{nm} = \det \begin{pmatrix} \delta_{nm} & U_m \\ U_n^\dagger & U^\dagger U \end{pmatrix} \quad (\text{A8})$$

where U_n is the n -th row of U . Using the well known identity $\det \begin{pmatrix} A & B \\ C & D \end{pmatrix} = \det D \det(A - BD^{-1}C)$ and exploiting the fact that $U^\dagger U$ is a submatrix of a unitary matrix one obtains

$$R_{nm} = \delta_{nm} - (U U^\dagger)_{nm}, \quad (\text{A9})$$

Thanks to Eq.(2), one can write $R_{nm}(t) = [\delta_{nm} + (-1)^m f_{nm}(2t)]/2$. Using (A5)

$$R_{nm}(t^*/2) = \frac{\delta_{nm} + (-1)^m (-i)^{N-1} \delta_{m, N-n+1}}{2}. \quad (\text{A10})$$

By imposing that (A10) and (A9) are equal one finds the simple solution

$$U_{nk}(t^*/2) = \begin{cases} \frac{\delta_{n,k} + e^{i\alpha n} \delta_{n, N-k+1}}{\sqrt{2}} & \text{if } k \neq N - k + 1, \\ 1 & \text{if } k = N - k + 1, \end{cases} \quad (\text{A11})$$

where $e^{i\alpha_n} = i^{N-1}(-1)^{n-1}$. Therefore, one obtains that

$$|\Xi\rangle = e^{-i\mathcal{H}_0 t^*/2} |\text{AFM}\rangle = \left(\frac{c_1^\dagger + e^{i\alpha_1} c_N^\dagger}{\sqrt{2}} \right) \left(\frac{c_2^\dagger + e^{i\alpha_2} c_{N-1}^\dagger}{\sqrt{2}} \right) \dots |0\rangle \quad (\text{A12})$$

for N even and

$$|\Xi\rangle = \left(\frac{c_1^\dagger + e^{i\alpha_1} c_N^\dagger}{\sqrt{2}} \right) \left(\frac{c_2^\dagger + e^{i\alpha_2} c_{N-1}^\dagger}{\sqrt{2}} \right) \dots c_{(N+1)/2}^\dagger |0\rangle \quad (\text{A13})$$

for N odd. Going back into the spin representation, exploiting the anti-commutation relations, one obtains that $|\Xi\rangle$ consists of a product of maximally entangled states, as in Fig. (1)

$$|\Xi\rangle_{\text{even}} = \prod_{k=1}^{N/2} \left(\frac{|\uparrow\downarrow\rangle_{k,\bar{k}} - i|\downarrow\uparrow\rangle_{k,\bar{k}}}{\sqrt{2}} \right) \quad (\text{A14})$$

$$|\Xi\rangle_{\text{odd}} = |\uparrow\rangle_{N/2} \prod_{k=1}^{N/2} \left(\frac{|\uparrow\downarrow\rangle_{k,\bar{k}} + |\downarrow\uparrow\rangle_{k,\bar{k}}}{\sqrt{2}} \right) \quad (\text{A15})$$

where $\bar{k} = N - k + 1$. A schematic picture of the resulting state is drawn in Fig. 1 in the main text.

Appendix B: Distance-independent entanglement generation

As stated in the main text, the Hamiltonian \mathcal{H}_0 can be expressed as a JW-fermionic hopping model

$$\mathcal{H}_0 = \sum_{n,m} \hat{c}_n^\dagger A_{n,m} \hat{c}_m, \quad (\text{B1})$$

where $A_{n,m} = j_n(\delta_{n,m+1} + \delta_{n+1,m})$. The hopping matrix A can be diagonalized with an orthogonal matrix g where $\sum_{i,j=1}^N g_{k,i} A_{i,j} g_{l,j} = E_k \delta_{k,l}$. The diagonalization was done analytically in Ref.[76]. Hence the fermionic operators in the Heisenberg picture are found to be $\hat{c}_k(t) = \sum_l f_{k,l} \hat{c}_l(0)$, $\hat{c}_k^\dagger(t) = \sum_l f_{k,l}^* \hat{c}_l^\dagger(0)$ where $f_{k,l}(t) = \sum_{m=1}^N g_{m,k} g_{m,l} e^{-iE_m t}$.

In the basis $\{|\uparrow\uparrow\rangle, |\uparrow\downarrow\rangle, |\downarrow\uparrow\rangle, |\downarrow\downarrow\rangle\}$, the only non-vanishing elements of the density matrix of the distant ends spins $\rho_{1,N}$ are

$$\rho_{1,N} = \begin{pmatrix} \rho_{11} & & & \\ & \rho_{22} & \rho_{23} & \\ & \rho_{32} & \rho_{33} & \\ & & & \rho_{44} \end{pmatrix}. \quad (\text{B2})$$

Defining

$$\alpha = \langle \hat{c}_1^\dagger(t) \hat{c}_1(t) \rangle, \beta = \langle \hat{c}_N^\dagger(t) \hat{c}_N(t) \rangle, \gamma = \langle \hat{c}_1^\dagger(t) \hat{c}_N(t) \rangle, \quad (\text{B3})$$

we find the density matrix elements to be

$$\begin{aligned} \rho_{11} &= \alpha\beta - |\gamma|^2, & \rho_{44} &= (1 - \alpha)(1 - \beta) - |\gamma|^2, \\ \rho_{22} &= \alpha(1 - \beta) + |\gamma|^2, & \rho_{33} &= \beta(1 - \alpha) + |\gamma|^2, \\ \rho_{23} &= (-1)^{M+1} \gamma^*, & \rho_{32} &= (-1)^{M+1} \gamma, \end{aligned} \quad (\text{B4})$$

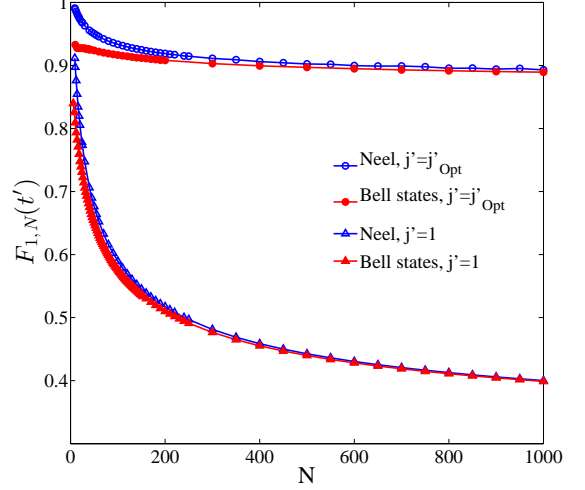


FIG. 5. (Color online) Maximum $F_{1,N}$ for the minimally engineered Hamiltonian versus the chain length.

where the two point correlation function is given by

$$\langle \hat{c}_i^\dagger(t) \hat{c}_j(t) \rangle = \sum_{m=\text{odd}} f_{i,m}^*(t) f_{j,m}(t) \langle \hat{c}_m^\dagger(0) \hat{c}_m(0) \rangle, \quad (\text{B5})$$

and M is the number of up spins in the initial state, i.e. $N/2$ for even N and $(N+1)/2$ for odd N . Having the analytic expression for the density matrix, we now evaluate the entanglement between spins 1 and N using the fully entanglement fraction F . For $\rho_{1,N}$ we find that

$$F_{1,N} = \max \left\{ \frac{\alpha\beta + (\alpha - 1)(\beta - 1)}{2} - |\gamma|^2, \frac{\alpha + \beta}{2} - \alpha\beta + |\gamma|(1 + |\gamma|) \right\}. \quad (\text{B6})$$

Substituting for α, β , and γ at half the transmission time into eq.(B6) we get the fully entangled fraction

$$F_{1,N}(t^*/2) = \frac{1}{4} (1 + |f_{1,N}(t^*)|^2). \quad (\text{B7})$$

From Ref. [45], $|f_{1,N}(t^*)|$ was found to approach an asymptotic value of 0.8469 for large N and hence the asymptotic value of the generated entanglement F in this work is 0.8528. The optimal time for entanglement generation from a quench would be half the time required for state transfer and hence $t^*/2 = \frac{1}{2J}(N + 2.29N^{1/3})$. The resulting $F_{1,N}$ is shown in Fig. 5 and compared with the case of a homogeneous XX Hamiltonian [30]. The time $t^*/2$ is shown in Fig. 6(a). Fig. 6(b) shows the reading time defined as the time interval where $F_{1,N} > F(t^*)/2$.

Fig. 7(a,b) shows the fully entangled fraction evaluated numerically for the mirror-symmetric spins in a chain of length $N = 10$ for the fully engineered and minimally engineered Hamiltonian considered in this article.

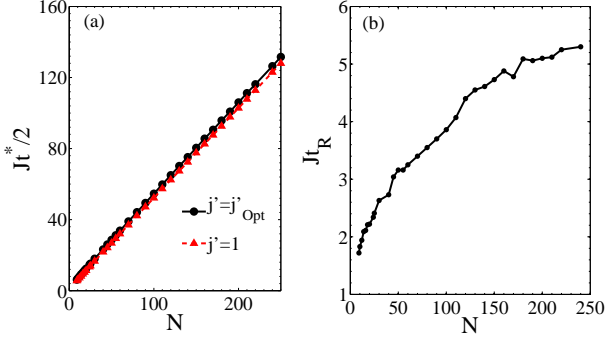


FIG. 6. (Color online) (a) Time at which the first peak of $F_{1,N}$ occurs versus the chain length for the minimally engineered Hamiltonian and Néel initial state (b) Reading time defined as the width of $F_{1,N}(t)$ at half the maximum.

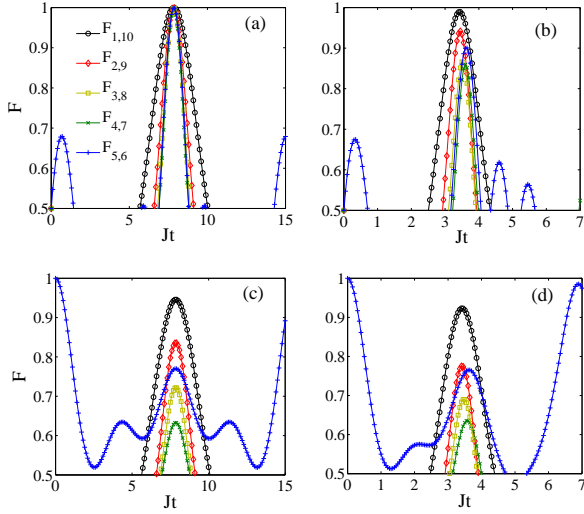


FIG. 7. (Color online) Fully entangled fraction for $N = 10$ for (a,b) Néel initial state with the fully engineered and minimally engineered Hamiltonian, respectively. (c,d) Series of Bell states initial state with the fully engineered and minimally engineered Hamiltonian, respectively.

Appendix C: Series of Bell States

We also consider the following product of Bell states as an initial state,

$$|\psi\rangle = \bigotimes_{k=1}^{N/2} |\psi_{k,k+1}\rangle = \bigotimes_{k=1}^{N/2} (|\uparrow_k \downarrow_{k+1}\rangle - |\downarrow_k \uparrow_{k+1}\rangle). \quad (\text{C1})$$

In this case, the density matrix elements $\rho_{1,N}$ is found to be

$$\begin{aligned} \rho_{11} &= \alpha\beta - |\gamma|^2, & \rho_{44} &= (1-\alpha)(1-\beta) - |\gamma|^2 \\ \rho_{22} &= \alpha(1-\beta) + |\gamma|^2, & \rho_{33} &= \beta(1-\alpha) + |\gamma|^2 \\ \rho_{23} &= \delta^*, & \rho_{32} &= \delta, \end{aligned} \quad (\text{C2})$$

where we defined

$$\begin{aligned} \alpha &= \langle \hat{c}_1^\dagger(t) \hat{c}_1(t) \rangle, \beta = \langle \hat{c}_N^\dagger(t) \hat{c}_N(t) \rangle, \gamma = \langle \hat{c}_1^\dagger(t) \hat{c}_N(t) \rangle, \\ \delta &= \sum_{l,m} f_{1,l}^*(t) f_{N,m}(t) \langle \hat{c}_m \hat{c}_l^\dagger \otimes_{i=1}^N (-\sigma_i^z) \rangle. \end{aligned} \quad (\text{C3})$$

The two point correlation functions are given by $\langle \hat{c}_i^\dagger(t) \hat{c}_j(t) \rangle = \sum_{l,m} f_{i,l}^*(t) f_{j,m}(t) \langle \hat{c}_l^\dagger \hat{c}_m \rangle$ where

$$\langle \hat{c}_l^\dagger \hat{c}_m \rangle = \begin{cases} \frac{1}{2}, & l = m \\ -\frac{1}{2}, & |l - m| = 1 \\ 0, & \text{otherwise} \end{cases} \quad (\text{C4})$$

and

$$\langle \hat{c}_l \hat{c}_m^\dagger \otimes_{i=1}^N (-\sigma_i^z) \rangle = \begin{cases} \frac{1}{2}(-1)^{N/2}, & l = m \\ \frac{1}{2}(-1)^{N/2}, & l = \text{odd}, m = l + 1 \\ \frac{1}{2}(-1)^{N/2}, & l = \text{even}, m = l - 1 \\ 0, & \text{otherwise} \end{cases} \quad (\text{C5})$$

we then find the fully entangled fraction of $\rho_{1,N}$

$$F_{1,N}(t) = \max \left\{ \frac{\alpha\beta + (\alpha-1)(\beta-1)}{2} - |\gamma|^2, \frac{\alpha+\beta}{2} - \alpha\beta + |\gamma|^2 \pm \delta \right\}. \quad (\text{C6})$$

The resulting $F_{1,N}$ are shown in Fig. 5 for two initial states: (i) Néel state and (ii) series of Bell states. Fig. 7 shows the fully entangled fraction evaluated numerically for the mirror-symmetric spins in a chain of length $N = 10$ for the fully engineered and minimally engineered Hamiltonian and the two initial states considered in this work.

- [1] C. H. Bennett, G. Brassard, C. Crpeau, R. Jozsa, A. Peres, and W. K. Wootters, *Physical Review Letters* **70**, 1895 (1993).
 [2] D. L. Moehring, P. Maunz, S. Olmschenk, K. C. Younge, D. N. Matsukevich, L.-M. Duan, and C. Monroe,

- Nature* **449**, 68 (2007).
 [3] D. Hucul, I. V. Inlek, G. Vittorini, C. Crocker, S. Debnath, S. M. Clark, and C. Monroe, arXiv:1403.3696 [quant-ph] (2014).
 [4] C. Weitenberg, S. Kuhr, K. Mlmer, and J. F. Sherson,

- Physical Review A **84**, 032322 (2011).
- [5] N. Yao, L. Jiang, A. Gorshkov, Z.-X. Gong, A. Zhai, L.-M. Duan, and M. Lukin, Physical Review Letters **106** (2011), 10.1103/PhysRevLett.106.040505.
- [6] L. Bianchi, A. Bayat, P. Verrucchi, and S. Bose, Physical Review Letters **106** (2011), 10.1103/PhysRevLett.106.140501.
- [7] Y. Ping, B. W. Lovett, S. C. Benjamin, and E. M. Gauger, Physical review letters **110**, 100503 (2013).
- [8] P. Calabrese and J. Cardy, Journal of Statistical Mechanics: Theory and Experiment **2005**, P04039 (2005).
- [9] G. De Chiara, S. Montangero, P. Calabrese, and R. Fazio, Journal of Statistical Mechanics: Theory and Experiment **2006**, P03001 (2006).
- [10] A. Das, S. Garnerone, and S. Haas, Physical Review A **84**, 052317 (2011).
- [11] P. Barmettler, A. Rey, E. Demler, M. Lukin, I. Bloch, and V. Gritsev, Phys. Rev. A **78**, 012330 (2008).
- [12] K. Sengupta and D. Sen, Physical Review A **80**, 032304 (2009).
- [13] G. Sadiq, B. Alkurtass, and O. Aldossary, Physical Review A **82**, 052337 (2010).
- [14] B. Alkurtass, G. Sadiq, and S. Kais, Physical Review A **84**, 022314 (2011).
- [15] G. Sadiq, Q. Xu, and S. Kais, arXiv preprint arXiv:1304.5569 (2013).
- [16] J. Eisert, M. B. Plenio, S. Bose, and J. Hartley, Physical review letters **93**, 190402 (2004).
- [17] J. Schachenmayer, B. Lanyon, C. Roos, and A. Daley, arXiv preprint arXiv:1305.6880 (2013).
- [18] P. Hauke and L. Tagliacozzo, Physical Review Letters **111**, 207202 (2013).
- [19] H. Kim and D. A. Huse, Physical Review Letters **111**, 127205 (2013).
- [20] J. H. Bardarson, F. Pollmann, and J. E. Moore, Physical Review Letters **109**, 017202 (2012).
- [21] M. Serbyn, Z. Papi, and D. A. Abanin, Physical Review Letters **110**, 260601 (2013).
- [22] R. Vosk and E. Altman, Physical Review Letters **110**, 067204 (2013).
- [23] P. Jurcevic, B. P. Lanyon, P. Hauke, C. Hempel, P. Zoller, R. Blatt, and C. F. Roos, arXiv:1401.5387 [cond-mat, physics:physics, physics:quant-ph] (2014).
- [24] P. Richerme, Z.-X. Gong, A. Lee, C. Senko, J. Smith, M. Foss-Feig, S. Michalakakis, A. V. Gorshkov, and C. Monroe, arXiv:1401.5088 [quant-ph] (2014).
- [25] T. Fukuhara, P. Schau, M. Endres, S. Hild, M. Cheneau, I. Bloch, and C. Gross, Nature **502**, 76 (2013).
- [26] L. Campos Venuti, C. Degli Esposti Boschi, and M. Roncaglia, Physical review letters **96**, 247206 (2006).
- [27] L. Campos Venuti, S. M. Giampaolo, F. Illuminati, P. Zanardi, and L. Campos Venuti, Physical Review A **76**, 52328 (2007).
- [28] S. M. Giampaolo and F. Illuminati, New Journal of Physics **12**, 25019 (2010).
- [29] S. Zippilli, M. Johanning, S. M. Giampaolo, C. Wunderlich, and F. Illuminati, arXiv preprint arXiv:1304.0261 (2013).
- [30] H. Wichterich and S. Bose, Phys. Rev. A **79**, 60302 (2009).
- [31] B. Alkurtass, H. Wichterich, and S. Bose, arXiv preprint arXiv:1309.5756 (2013).
- [32] A. Bayat, S. Bose, and P. Sodano, Physical Review Letters **105**, 187204 (2010).
- [33] P. Sodano, A. Bayat, and S. Bose, Physical Review B **81**, 100412 (2010).
- [34] A. Bayat, L. Bianchi, S. Bose, and P. Verrucchi, Physical Review A **83** (2011), 10.1103/PhysRevA.83.062328.
- [35] L. Sansoni, F. Sciarrino, G. Vallone, P. Mataloni, A. Crespi, R. Ramponi, and R. Osellame, Physical Review Letters **108**, 010502 (2012).
- [36] S. Aaronson and A. Arkhipov, in *Proceedings of the Forty-third Annual ACM Symposium on Theory of Computing*, STOC '11 (ACM, New York, NY, USA, 2011) p. 333342.
- [37] B. M. Terhal and D. P. DiVincenzo, Physical Review A **65**, 032325 (2002).
- [38] M. Cheneau, P. Barmettler, D. Poletti, M. Endres, P. Schau, T. Fukuhara, C. Gross, I. Bloch, C. Kollath, and S. Kuhr, Nature **481**, 484 (2012).
- [39] S. Bose, Physical review letters **91**, 207901 (2003).
- [40] A. M. Childs, Physical Review Letters **102**, 180501 (2009).
- [41] A. M. Childs, International Journal of Quantum Information **08**, 641 (2010).
- [42] C. Di Franco, M. Paternostro, and M. S. Kim, Physical Review A **77**, 020303 (2008).
- [43] L. Bianchi, The European Physical Journal Plus **128**, 1 (2013).
- [44] L. Bianchi, T. Apollaro, A. Cuccoli, R. Vaia, and P. Verrucchi, Physical Review A **82** (2010), 10.1103/PhysRevA.82.052321.
- [45] L. Bianchi, T. J. G. Apollaro, A. Cuccoli, R. Vaia, and P. Verrucchi, New Journal of Physics **13**, 123006 (2011).
- [46] S. Bose, A. Bayat, P. Sodano, L. Bianchi, and P. Verrucchi, in *Quantum State Transfer and Network Engineering*, Quantum Science and Technology, edited by G. M. Nikolopoulos and I. Jex (Springer Berlin Heidelberg, 2014) pp. 1–37.
- [47] A. Koetsier, R. Duine, I. Bloch, and H. Stoof, Phys. Rev. A **77**, 023623+ (2008).
- [48] E. H. Lieb, Physical Review **162**, 162172 (1967).
- [49] M. Christandl, N. Datta, A. Ekert, and A. J. Landahl, Physical review letters **92**, 187902 (2004).
- [50] A. Kay, Arxiv preprint arXiv:0903.4274 (2009).
- [51] C. H. Bennett, D. P. DiVincenzo, J. A. Smolin, and W. K. Wootters, Physical Review A **54**, 38243851 (1996).
- [52] S. Trotzky, Y.-A. Chen, U. Schnorrberger, P. Cheinet, and I. Bloch, (2010).
- [53] C. Negrevergne, T. S. Mahesh, C. A. Ryan, M. Ditty, F. Cyr-Racine, W. Power, N. Boulant, T. Havel, D. G. Cory, and R. Laflamme, Physical Review Letters **96**, 170501 (2006).
- [54] P. Cappellaro, in *Quantum State Transfer and Network Engineering*, Quantum Science and Technology, edited by G. M. Nikolopoulos and I. Jex (Springer Berlin Heidelberg, 2014) pp. 183–222.
- [55] K. R. K. Rao, T. S. Mahesh, and A. Kumar, arXiv:1307.5220 [quant-ph] (2013).
- [56] W. Zhang, P. Cappellaro, N. Antler, B. Pepper, D. G. Cory, V. V. Dobrovitski, C. Ramanathan, and L. Viola, Physical Review A **80**, 052323 (2009).
- [57] A. Ajoy and P. Cappellaro, Physical Review Letters **110**, 220503 (2013).
- [58] D. G. Cory, A. F. Fahmy, and T. F. Havel, Proceedings of the National Academy of Sciences **94**, 1634 (1997).
- [59] N. A. Gershenfeld and I. L. Chuang, Science **275**, 350 (1997).
- [60] E. Knill and R. Laflamme, Phys. Rev. A **55**, 900911 (1997).
- [61] G. Kaur and P. Cappellaro, New Journal of Physics **14**, 083005 (2012).
- [62] D. Mc Hugh and J. Twamley, Physical Review A **71**, 012315 (2005).
- [63] M. Johanning, A. F. Varn, and C. Wunderlich, Journal of Physics B: Atomic, Molecular and Optical Physics **42**, 154009 (2009).
- [64] A. Khromova, C. Piltz, B. Scharfenberger, T. F. Gloger, M. Johanning, A. F. Varn, and C. Wunderlich, Physical Review Letters **108**, 220502 (2012).
- [65] C. Wunderlich, in *Laser Physics at the Limits*, edited by D. H. Figger, P. D. C. Zimmermann, and P. D. D. Meschede (Springer Berlin Heidelberg, 2002) pp. 261–273.
- [66] H. Wunderlich, C. Wunderlich, K. Singer, and F. Schmidt-

- Kaler, Physical Review A **79**, 052324 (2009).
- [67] D. Porras and J. I. Cirac, Physical Review Letters **92**, 207901 (2004).
- [68] C. Piltz, B. Scharfenberger, A. Khromova, A. F. Varn, and C. Wunderlich, Physical Review Letters **110**, 200501 (2013).
- [69] K. Kim, M.-S. Chang, R. Islam, S. Korenblit, L.-M. Duan, and C. Monroe, Physical Review Letters **103**, 120502 (2009).
- [70] M. Lubasch, V. Murg, U. Schneider, J. I. Cirac, and M.-C. Bauls, Physical Review Letters **107**, 165301 (2011).
- [71] S. Trotzky, P. Cheinet, S. Fölling, M. Feld, U. Schnorrberger, A. M. Rey, A. Polkovnikov, E. A. Demler, M. D. Lukin, and I. Bloch, Science **319**, 295 (2008).
- [72] T. Fukuhara, A. Kantian, M. Endres, M. Cheneau, P. Schau, S. Hild, D. Bellem, U. Schollwck, T. Giamarchi, C. Gross, I. Bloch, and S. Kuhr, Nature Physics **9**, 235 (2013).
- [73] S. R. Clark, C. Moura Alves, and D. Jaksch, New Journal of Physics **7**, 124 (2005).
- [74] L. M. Duan, E. Demler, and M. D. Lukin, Physical review letters **91**, 90402 (2003).
- [75] L. Biedenharn and J. D. Louck, *Angular Momentum in Quantum Physics: Theory and Application, Encyclopedia of Mathematics and its Applications* (Addison-Wesley, Englewood Cliffs, 1981).
- [76] L. Banchi and R. Vaia, Journal of Mathematical Physics **54**, 43501 (2013).